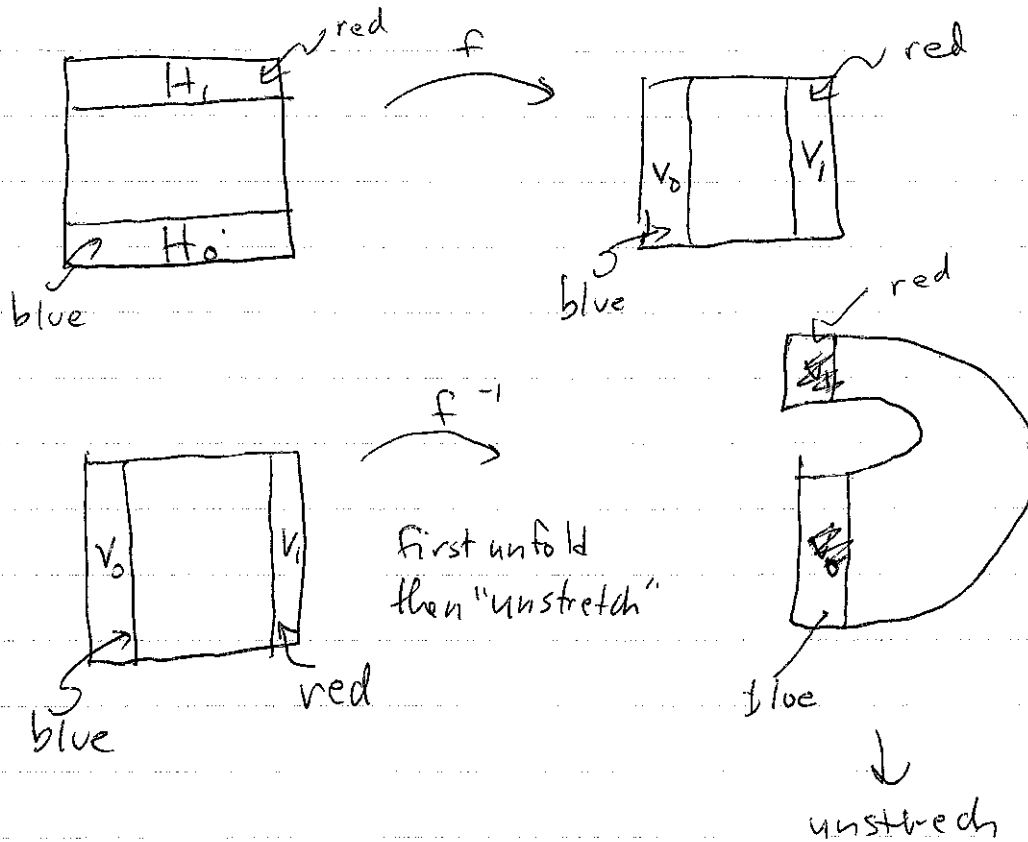
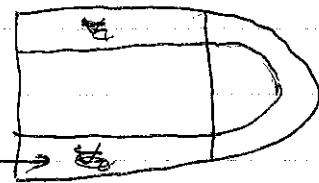


Small horseshoe:

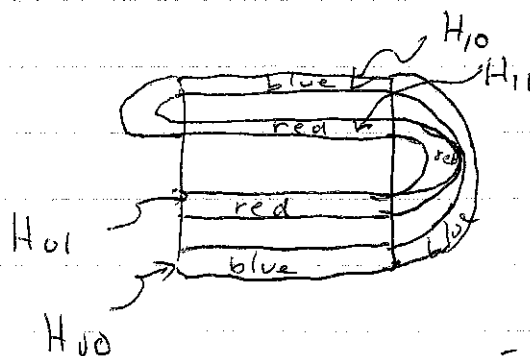


$$H_1 = f^{-1}(V_1)$$

$$H_0 = f^{-1}(V_0)$$



repeat



$$D \cap f^{-1}(D) \cap f^{-2}(D)$$

$$= \bigcup_{s_i \in S} H_{s_0 s_i}$$

$$= \left\{ p \in H_{s_0}, f(p) \in H_{s_1}, s_i \in \{0, 1\}, i = 0, 1 \right\}$$

$$\Lambda = \text{invariant set} = \bigcap_{n=-\infty}^{+\infty} f^n(D)$$

= set of pts in intersection of vertical lines $V_{S_{-1}S_{-2}\dots}$ & horizontal lines $H_{S_0S_1\dots}$

$p \mapsto \underbrace{\dots S_{-k} \dots S_{-2} S_{-1}}_{\text{labels vertical strips (f map, the past)}} \circ \underbrace{S_0 S_1 \dots S_k \dots}_{\text{labels horizontal strips (f^{-1} map, the future)}}$

if $S = \dots S_{-k} \dots S_{-1} \circ S_0 S_1 \dots S_k \dots$

then $\sigma(S) = \dots S_{-k} \dots S_{-1} S_0 \circ S_1 \dots S_k \dots$

\nearrow
gives us $f(p)$

Thm. Shift map σ acting on space of bi-infinite sequence of 0's & 1's has

(i) countable set of periodic orbits of arbitrarily high periods \leftarrow repeating sequences

(ii) uncountably infinite set of nonperiodic orbits \leftarrow nonrepeating

(iii) a dense orbit \nwarrow

(last dense orbit on ~~shift~~

map $x_{n+1} = 2x_n \pmod{1}$)

example from ODEs where Smale horseshoe arises
 "homoclinic tangle" (p. 302 in text - quote from Poincaré)

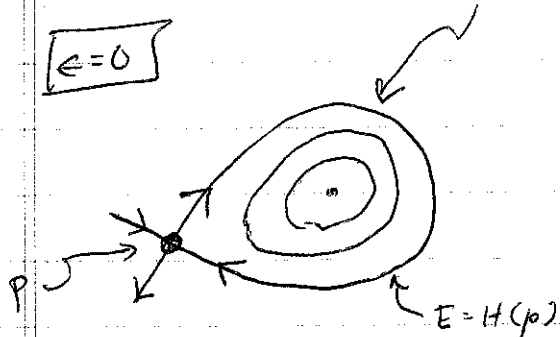
$(x, y) \in \mathbb{R}^2$ but with time-dependent perturbation

$$\dot{x} = \frac{\partial H}{\partial y}(x, y) + \epsilon g_1(x, y, t; \epsilon) \quad \leftarrow \epsilon \ll 1$$

$$\dot{y} = -\frac{\partial H}{\partial x}(x, y) + \epsilon g_2(x, y, t; \epsilon) \quad \leftarrow \begin{matrix} g_i \text{ is} \\ T\text{-periodic} \end{matrix}$$

$\epsilon = 0 \Rightarrow$ Hamiltonian system with conserved quantity $H(x_0, y_0) = E_0$

assume for $\epsilon = 0$, that there is a saddle-pt p_s with a homoclinic orbit



re-write nonautonomous ($\epsilon \neq 0$) problem as an autonomous one on $\mathbb{R}^2 \times S^1$

$$q = (x, y) \in \mathbb{R}^2 \quad \uparrow \quad \mathbb{R}^2 \times S^1 \quad \leftarrow \begin{matrix} \phi = \omega t \\ \text{identify } \phi = 0 \text{ \& } \phi = 2\pi \end{matrix} \quad \omega = \frac{2\pi}{T}$$

$$\dot{q} = J \nabla H + \epsilon g(q, \phi; \epsilon)$$

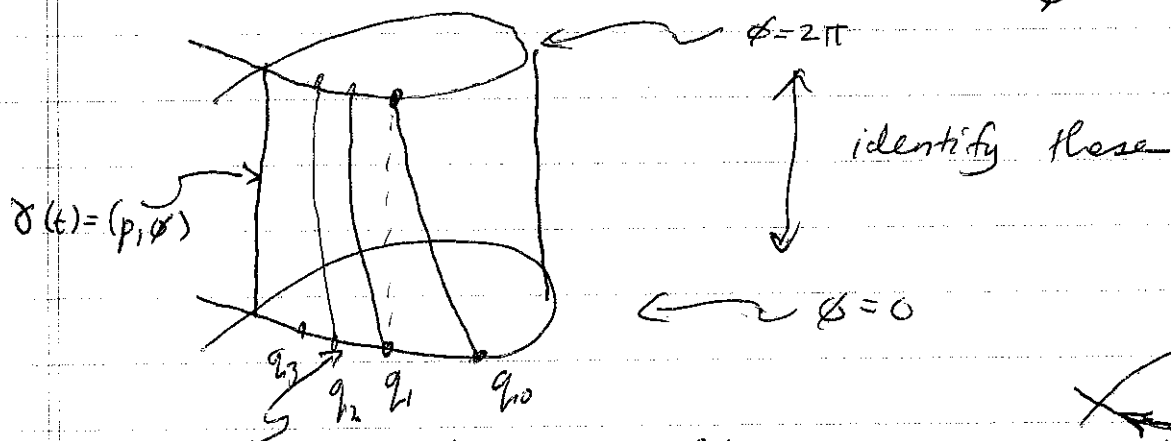
$$\dot{\phi} = \omega$$

$$J = \begin{pmatrix} 0 & 1 \\ -1 & 0 \end{pmatrix}, \quad \nabla H = \begin{pmatrix} \partial H / \partial x \\ \partial H / \partial y \end{pmatrix}$$

$\epsilon=0$

$$\left. \begin{aligned} \dot{q} &= J \nabla H \\ \dot{\phi} &= \omega \end{aligned} \right\}$$

~~right~~ this doesn't depend on ϕ



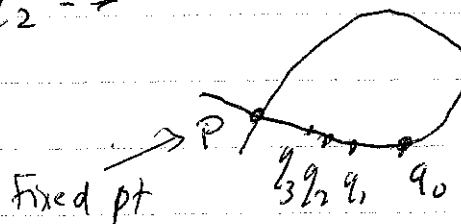
2-dim homoclinic manifold to the periodic orbit $\gamma(t)$

in q -plane with $\phi(t) = \omega t \pmod{2\pi}$

in terms of "stroboscopic map"

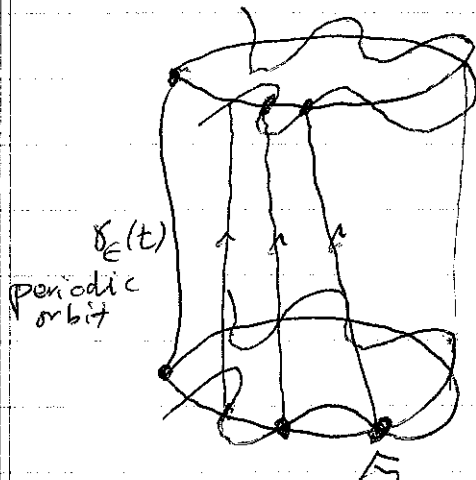
$$\text{i.e. } (q_0, \phi_0=0) \mapsto (q_1, \phi_1=2\pi)$$

$$q_0 \rightarrow q_1 \rightarrow q_2 \rightarrow \dots$$



iterates of 2-d map

$\epsilon \neq 0$: a generic possibility - the 2d stable & unstable manifolds of $\gamma_\epsilon(t)$ have a 1-d intersection

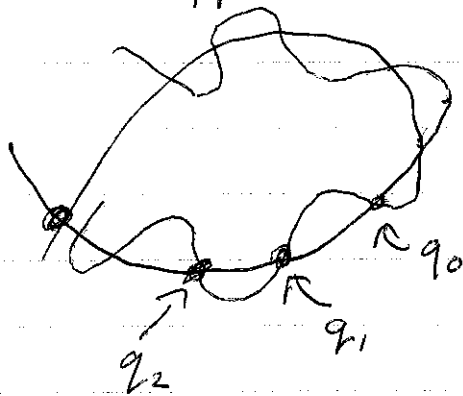


$W^s(\gamma_e(t))$ blue

$W^u(\gamma_e(t))$ red

one soln. in the 1-dim homoclinic manifold

as 2-d map



$$q_{n+1} = F(q_n)$$

\Rightarrow Wiggins

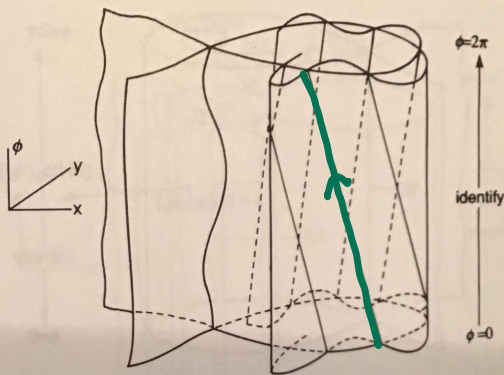
**Texts in
Applied
Mathematics
2**

S. Wiggins

Introduction to Applied Nonlinear Dynamical Systems and Chaos

4.5. Melnikov's Method for Homoclinic Orbits

487



Γ intersects
of
manifolds

FIGURE 4.5.3.

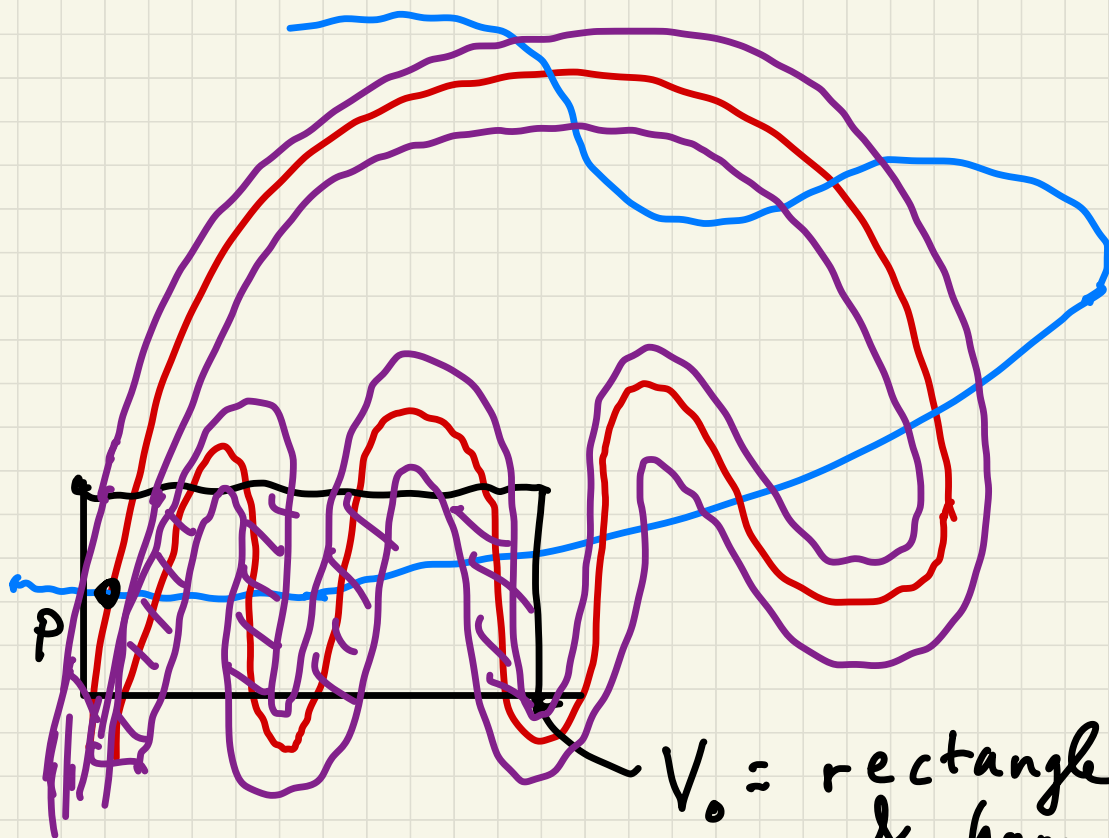
the distance between the perturbed stable and unstable manifolds along the direction normal to Γ_γ . Evidently, this measurement will vary from point-to-point on Γ_γ so we first need to describe a parametrization of Γ_γ .

Parametrization of Γ_γ : Homoclinic Coordinates. Every point on Γ_γ can be represented by

$$(q_0(-t_0), \phi_0) \in \Gamma_\gamma$$

(4.5.9)

ation of t_0 is the time of flight from
perturbed homoclinic



$W^u(p)$

$W^s(p)$

V_0 = rectangle containing p
& homoclinic pts

image of V_0 after some n
iterations of map, n large enough

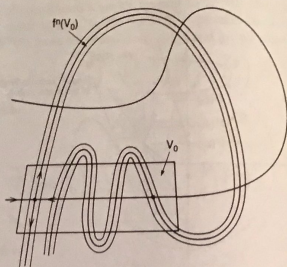


FIGURE 4.4.9.

Again, as a result of the lambda lemma, for N_0 sufficiently large, $|\eta_{f^n}(x_0)|$ can be made arbitrarily large, $|\xi_{f^n}(x_0)|$ can be made arbitrarily small, and by transversality of the intersection of $W^u(0)$ and $W^s(0)$ at g , $d \neq 0$ (with ϕ_{10} small compared to d). Thus, (4.4.29) can be made as large as we desire by choosing N_0 big enough.

The Smale-Birkhoff Homoclinic Theorem

The Smale-Birkhoff homoclinic theorem is very similar to Moser's theorem. We will state the theorem and describe briefly how it differs. The assumptions and set-up are the same as for Moser's theorem.

Theorem 4.4.3 (Smale [1963]) *There exists an integer $n \geq 1$ such that f^n has an invariant Cantor set on which it is topologically conjugate to a full shift on N symbols.*

Proof: We will only give the barest outline in order to show the difference between the Smale-Birkhoff homoclinic theorem and Moser's theorem and leave the details as an exercise for the reader (Exercise 4.8).

Choose a "rectangle," V_0 , containing a homoclinic point and the hyperbolic fixed point as shown in Figure 4.4.9. Then, for n sufficiently large, $f^n(V_0)$ intersects V_0 a finite number of times as shown in Figure 4.4.9. Now, one can find μ_k -horizontal strips in V_0 that map over themselves in μ_k -vertical strips such that Assumptions 1 and 3 of Section 4.3 hold; see Figure 4.4.10. The details needed to prove these statements are very similar to those needed for the proof of Moser's theorem, and it will be an instructive exercise for the reader to give a rigorous proof. \square

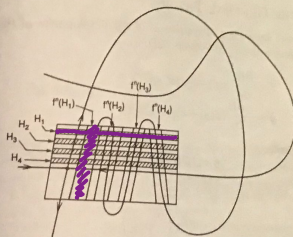


FIGURE 4.4.10. Horizontal strips H_1, \dots, H_k and their image under f^n .

From the outline of the proof of the Smale-Birkhoff homoclinic theorem, one can see how it differs from Moser's theorem. In both cases the invariant Cantor set is constructed near a homoclinic point sufficiently close to the hyperbolic fixed point. However, in the Smale-Birkhoff theorem, all points leave the Cantor set and return at the same time (i.e., after n iterates of f); in Moser's construction, points leave the Cantor set and may return at different times (recall the definition of f^t). What are the dynamical consequences of the two different constructions (see Exercise 4.9)?

4.5 Melnikov's Method for Homoclinic Orbits in Two-Dimensional, Time-Periodic Vector Fields

We have seen that transverse homoclinic orbits to hyperbolic periodic points of two-dimensional maps gives rise to chaotic dynamics in the sense of Theorems 4.4.2 and 4.4.3. We will now develop a perturbation method originally due to Melnikov [1963] for proving the existence of transverse homoclinic orbits to hyperbolic periodic orbits in a class of two-dimensional, time-periodic vector fields; then by considering a Poincaré map, Theorems 4.4.2 and 4.4.3 can be applied to conclude that the system possesses chaotic dynamics.

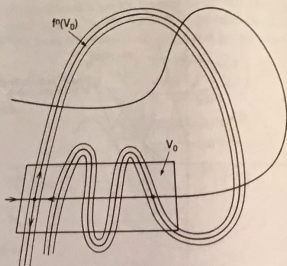


FIGURE 4.4.9.

Again, as a result of the lambda lemma, for N_0 sufficiently large, $|\eta f^n(r_{(n)})|$ can be made arbitrarily large, $|\xi f^n(r_{(n)})|$ can be made arbitrarily small, and by transversality of the intersection of $W^u(0)$ and $W^s(0)$ at q , $d \neq 0$ (with ϕ_{15} small compared to d). Thus, (4.4.29) can be made as large as we desire by choosing N_0 big enough.

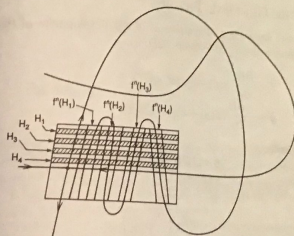
The Smale-Birkhoff Homoclinic Theorem

The Smale-Birkhoff homoclinic theorem is very similar to Moser's theorem. We will state the theorem and describe briefly how it differs. The assumptions and set-up are the same as for Moser's theorem.

Theorem 4.4.3 (Smale [1963]) *There exists an integer $n \geq 1$ such that f^n has an invariant Cantor set on which it is topologically conjugate to a full shift on N symbols.*

Proof: We will only give the barest outline in order to show the difference between the Smale-Birkhoff homoclinic theorem and Moser's theorem and leave the details as an exercise for the reader (Exercise 4.8).

Choose a "rectangle," V_0 , containing a homoclinic point and the hyperbolic fixed point as shown in Figure 4.4.9. Then, for n sufficiently large, $f^n(V_0)$ intersects V_0 a finite number of times as shown in Figure 4.4.9. Now, one can find μ_h -horizontal strips in V_0 that map over themselves in μ_s -vertical strips such that Assumptions 1 and 3 of Section 4.3 hold; see Figure 4.4.10. The details needed to prove these statements are very similar to those needed for the proof of Moser's theorem, and it will be an instructive exercise for the reader to give a rigorous proof. \square

FIGURE 4.4.10. Horizontal strips H_1, \dots, H_4 and their image under f^n .

From the outline of the proof of the Smale-Birkhoff homoclinic theorem, one can see how it differs from Moser's theorem. In both cases the invariant Cantor set is constructed near a homoclinic point sufficiently close to the hyperbolic fixed point. However, in the Smale-Birkhoff theorem, all points leave the Cantor set and return at the same time (i.e., after n iterates of f); in Moser's construction, points leave the Cantor set and may return at different times (recall the definition of f^T). What are the dynamical consequences of the two different constructions (see Exercise 4.9)?

4.5 Melnikov's Method for Homoclinic Orbits in Two-Dimensional, Time-Periodic Vector Fields

We have seen that transverse homoclinic orbits to hyperbolic periodic points of two-dimensional maps gives rise to chaotic dynamics in the sense of Theorems 4.4.2 and 4.4.3. We will now develop a perturbation method originally due to Melnikov [1963] for proving the existence of transverse homoclinic orbits to hyperbolic periodic orbits in a class of two-dimensional, time-periodic vector fields; then by considering a Poincaré map, Theorems 4.4.2 and 4.4.3 can be applied to conclude that the system possesses chaotic dynamics.